

# Dinuclear manganese(II) complexes of an acyclic phenol-based dinucleating ligand with four methoxyethyl chelating arms: synthesis, structure, magnetism and electrochemistry

Hiroshi Sakiyama <sup>a,\*</sup>, Akihiko Sugawara <sup>a</sup>, Masatomi Sakamoto <sup>a</sup>, Kei Unoura <sup>a</sup>,  
Katsuya Inoue <sup>b</sup>, Mikio Yamasaki <sup>c</sup>

<sup>a</sup> Department of Material and Biological Chemistry, Faculty of Science, Yamagata University, Kojirakawa, Yamagata 990-8560, Japan

<sup>b</sup> Institute for Molecular Science, Myodaiji, Okazaki 444-8585, Japan

<sup>c</sup> X-Ray Research Laboratory, Rigaku Corporation, 3-9-12 Matsubara, Akishima, Tokyo 196-8666, Japan

Received 11 May 2000; accepted 7 August 2000

## Abstract

Dinuclear manganese(II) complexes  $[\text{Mn}_2(\text{bomp})(\text{PhCO}_2)_2]\text{BPh}_4$  (**1**),  $[\text{Mn}_2(\text{bomp})(\text{MeCO}_2)_2]\text{BPh}_4$  (**2**), and  $[\text{Mn}_2(\text{bomp})(\text{PhCO}_2)_2]\text{PF}_6$  (**3**) were synthesized with a dinucleating ligand 2,6-bis[bis(2-methoxyethyl)aminomethyl]-4-methylphenol [H(bomp)]. Dinuclear zinc complex  $[\text{Zn}_2(\text{bomp})(\text{PhCO}_2)_2]\text{PF}_6$  (**4**) was also synthesized for the purpose of comparison. X-ray analysis revealed that the complex **1**·CHCl<sub>3</sub> contains two manganese ions bridged by the phenolic oxygen and two benzoate groups, forming a  $\mu$ -phenoxo-bis( $\mu$ -benzoato)dimanganese(II) core. Magnetic susceptibility measurements of **1–3** over the temperature range 1.8–300 K indicated antiferromagnetic interaction ( $J = -4$  to  $-6 \text{ cm}^{-1}$ ). Cyclic voltammograms of **3** showed a quasi-reversible oxidation process at +0.9 V versus a saturated sodium chloride calomel reference electrode, assigned to  $\text{Mn}^{\text{II}}\text{Mn}^{\text{II}}/\text{Mn}^{\text{II}}\text{Mn}^{\text{III}}$ . © 2000 Elsevier Science B.V. All rights reserved.

**Keywords:** Dinucleating ligand; Dinuclear manganese(II) complexes; Crystal structures; Magnetism; Electrochemistry

## 1. Introduction

Dinuclear manganese cores are often seen in biological systems, such as manganese catalases [1–4], manganese ribonucleotide reductase [5], arginase [6], thiosulfate oxidase [7], xylose isomerase [8], RNAase [9] and proline aminopeptidase [10]. The dimanganese cores exist as the catalytic centers of these enzymes. Some hydrolyze substrates by the ‘two-metal ion mechanism’, and some work as electron mediators to catalyze redox reactions. Manganese catalase is a well-studied redox enzyme that decomposes hydrogen peroxide. Manganese catalases have been isolated from four origins: *Lactobacillus plantarum* [1], *Thermoleophilum album* [2], *Thermus thermophilus* HB8 [3] and *Thermus* species strain YS 8-13 [4]. They catalyze

the disproportionation of  $\text{H}_2\text{O}_2$  to  $\text{O}_2$  and  $\text{H}_2\text{O}$ , and each subunit contains a dinuclear manganese core as its catalytic center. The dimanganese core works as a two-electron mediator between an  $\{\text{Mn}(\text{III})\}_2$  form and a reduced  $\{\text{Mn}(\text{II})\}_2$  form in  $\text{H}_2\text{O}_2$  disproportionation.

A great number of dinuclear manganese complexes have been synthesized and characterized as the model compounds of manganese enzymes. Among them, many complexes using macrocyclic or acyclic dinucleating ligands have been synthesized in order to stabilize the dimanganese core even in a reaction solution. 2,6-Bis[bis(2-pyridylmethyl)aminomethyl]-4-methylphenol [H(bpmp)] is one of the most well-known acyclic dinucleating ligands, and syntheses of dimanganese(II,II) complexes  $[\text{Mn}_2\text{bpmp}(\text{RCO}_2)_2]\text{ClO}_4$  ( $\text{R} = \text{Me}, \text{Ph}$ ) and dimanganese(II,III) complexes  $[\text{Mn}_2\text{bpmp}(\text{RCO}_2)_2](\text{ClO}_4)_2$  ( $\text{R} = \text{Me}, \text{Ph}$ ) have been reported [11] as frontier work in this research area.

In this study, the acyclic dinucleating ligand 2,6-bis[bis(2-methoxyethyl)aminomethyl]-4-methylphenol

\* Corresponding author. Fax: +81-23-628 4591.

E-mail address: saki@sci.kj.yamagata-u.ac.jp (H. Sakiyama).

[H(bomp)] is used to synthesize dimanganese complexes. This ligand is expected to stabilize dinuclear metal cores, and dizinc(II) complex  $[Zn_2\text{bomp}(\text{MeCO}_2)_2]\text{BPh}_4$  has been reported as a functional model of dizinc aminopeptidases [12]. Dinucleating ligands  $\text{bomp}^-$  and  $\text{bomp}^-$  will produce topologically the same chelating structures, but they are different in some aspects in regard to the nature of pyridyl and methoxy groups in their chelating arms. It is of interest to compare the properties of dimanganese complexes of  $\text{bomp}^-$  and  $\text{bomp}^-$ . Here we report the synthesis, structure, magnetism and electrochemical properties of dimanganese(II) complexes of  $\text{bomp}^-$  (Scheme 1).

## 2. Experimental

### 2.1. Measurements

Elemental analyses were obtained at the Elemental Analysis Service Centre of Kyushu University. Infrared (IR) spectra were recorded on a Hitachi 270-50 spectrometer, fast atom bombardment (FAB) mass spectra on a Fisons ZabSpec Q mass spectrometer in *N,N*-dimethylformamide (dmf) with a glycerol matrix, molar conductances on a DKK AOL-10 conductivity meter at room temperature, and electronic spectra on a Shimadzu UV-240 spectrometer. Magnetic susceptibility was measured between 1.8 and 300 K by using a Quantum Design SQUID magnetometer MPMS-5S in fields up to 5 T. Polycrystalline samples ( $\sim 30$  mg) were placed in a Japanese pharmacopoeia # 5 gel capsule. The background data of the capsule were measured separately and subtracted from the sample-in-cell data. Effective magnetic moments were calculated using the equation  $\mu_{\text{eff}} = (3kT\chi_{\text{M}}/N\beta^2)^{1/2}$ , where the symbols have their usual meanings. Voltammetric measurements were performed using an HECS-312B polarographic analyzer coupled with an HECS-321B function generator from Huso Co. Measurements were carried out in acetonitrile using a three-electrode cell consisting of a glassy carbon disk working electrode, platinum coil auxiliary electrode and a saturated sodium chloride

calomel electrode (SSCE) as reference. Tetra-*n*-butylammonium tetrafluoroborate was used as the supporting electrolyte. Thin-layer coulometry was accomplished using an HECS-978 Coulometer (Huso Co.) with a thermostatically controlled thin-layer electrochemical cell.

### 2.2. Materials

Na(bomp) was prepared by the method reported previously [12]. All chemicals were commercial products and were used as supplied.

### 2.3. Preparations

#### 2.3.1. $[Mn_2(\text{bomp})(\text{PhCO}_2)_2]\text{BPh}_4$ (**1**)

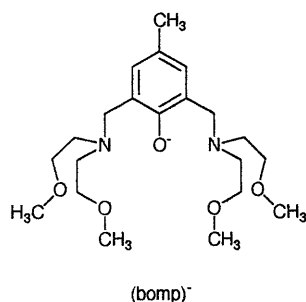
To a methanolic solution (10 ml) of manganese(II) benzoate tetrahydrate (0.74 g, 2.0 mmol) was added a methanolic solution (5 ml) of Na(bomp) (0.42 g, 1.0 mmol), and the resulting solution was refluxed for 1 h to give a yellow solution. The addition of a methanolic solution (5 ml) of sodium tetraphenylborate (0.34 g, 1.0 mmol) resulted in the precipitation of white microcrystals. Yield 0.34 g (32%) (Found: C, 66.35; H, 6.40; Mn, 11.0; N, 2.60. Calc. for  $C_{59}H_{67}BMn_2N_2O_9$ : C, 66.30; H, 6.30; Mn, 10.3; N, 2.60%). Selected IR data [ $\nu/\text{cm}^{-1}$ ] using KBr disk: 3050–2950, 1600, 1560, 1470, 1400, 1320, 1270, 1080, 1020–1000, 700. FAB mass spectrum;  $m/z$  749  $[Mn_2(\text{bomp})(\text{PhCO}_2)_2]^+$ . Molar conductance [ $A_M/S \text{ cm}^2 \text{ mol}^{-1}$ ] in dmf: 38.

#### 2.3.2. $[Mn_2(\text{bomp})(\text{MeCO}_2)_2]\text{BPh}_4$ (**2**)

This was prepared as white microcrystals by a method similar to that of **1** using manganese(II) acetate tetrahydrate instead of manganese(II) benzoate tetrahydrate. Yield 0.31 g (33%) (Found: C, 62.30; H, 6.70; Mn, 11.6; N, 2.95. Calc. for  $C_{49}H_{63}BMn_2N_2O_9$ : C, 62.30; H, 6.70; Mn, 11.5; N, 2.95%). Selected IR data [ $\nu/\text{cm}^{-1}$ ] using KBr disk: 3050–2950, 1590, 1470, 1420, 1320, 1270, 1080, 1020–1000, 730, 700. FAB mass spectrum;  $m/z$  625  $[Mn_2(\text{bomp})(\text{MeCO}_2)_2]^+$ . Molar conductance [ $A_M/S \text{ cm}^2 \text{ mol}^{-1}$ ] in dmf: 41.

#### 2.3.3. $[Mn_2(\text{bomp})(\text{PhCO}_2)_2]\text{PF}_6$ (**3**)

This was prepared as white microcrystals by a method similar to that of **1** using ammonium hexafluorophosphate instead of sodium tetraphenylborate. Yield 0.42 g (48%) (Found: C, 47.00; H, 5.30; N, 3.20. Calc. for  $C_{35}H_{47}F_6Mn_2N_2O_9P$ : C, 47.00; H, 5.30; N, 3.15%). Selected IR data [ $\nu/\text{cm}^{-1}$ ] using KBr disk: 2950–2900, 1610, 1560, 1480, 1400, 1320, 1280, 1090, 830, 720. FAB mass spectrum;  $m/z$  749  $[Mn_2(\text{bomp})(\text{PhCO}_2)_2]^+$ . Molar conductance [ $A_M/S \text{ cm}^2 \text{ mol}^{-1}$ ] in dmf: 63.



Scheme 1.

### 2.3.4. $[\text{Zn}_2(\text{bomp})(\text{PhCO}_2)_2]\text{PF}_6$ (**4**)

This was prepared as white microcrystals by a method similar to that of **3** using zinc(II) benzoate instead of manganese(II) benzoate tetrahydrate. Yield 0.09 g (8%) (Found: C, 45.95; H, 5.15; N, 3.10. Calc. for  $\text{C}_{35}\text{H}_{47}\text{F}_6\text{N}_2\text{O}_9\text{PZn}_2$ : C, 45.90; H, 5.15; N, 3.05%). Selected IR data [ $\nu/\text{cm}^{-1}$ ] using KBr disk: 2950–2850, 1610, 1570, 1480, 1400, 1320, 1270, 1090, 840, 720.  $^1\text{H}$  NMR [ $\delta/\text{ppm}$ ] in  $\text{CDCl}_3$ : 2.22 (s, 3H), 2.8–4.2 (br, 32H), 6.94 (s, 2H), 7.40 (t, 4H), 7.48 (t, 2H), 8.03 (d, 4H).  $^{13}\text{C}$  NMR [ $\delta/\text{ppm}$ ] in  $\text{CDCl}_3$ : 20.28, 59.54 (br), 61.98, 67.80 (br), 123.37, 126.56, 128.11, 129.70, 131.69, 132.09, 134.94, 159.93, 172.96. FAB mass spectrum;  $m/z$  767, 769, 771  $[\text{Zn}_2(\text{bomp})(\text{PhCO}_2)_2]^+$ . Molar conductance [ $\Lambda_{\text{M}}/\text{S cm}^2 \text{mol}^{-1}$ ] in dmf: 64.

### 2.4. Single crystal X-ray analysis of complex $1 \cdot \text{CHCl}_3$

Single crystals of complex  $1 \cdot \text{CHCl}_3$  were obtained by the slow diffusion of propan-2-ol into a chloroform solution of **1**. A colorless platelet crystal having approximate dimensions  $0.45 \times 0.20 \times 0.20 \text{ mm}^3$  was mounted in a glass capillary. All measurements were made on a Rigaku RAXIS–RAPID Imaging Plate diffractometer with graphite-monochromated Mo  $K\alpha$  radiation ( $\lambda = 0.71069 \text{ \AA}$ ). The data were collected at  $23 \pm 1^\circ\text{C}$  to a maximum  $2\theta$  value of  $55.0^\circ$ . Of the 54 071 reflections collected, 13 708 were unique ( $R_{\text{int}} = 0.034$ ). The data were corrected for Lorentz and polarization effects.

The structure was solved by direct methods [13] and expanded using Fourier techniques [14]. Hydrogen atoms were included but not refined. Refinement was carried out by the full-matrix least-squares method, where the function minimized was  $\sum w(|F_o| - |F_c|)^2$ . The final cycle of the refinement was based on 6583 observed reflections [ $I > 3.00\sigma(I)$ ], and the final values of  $R$  and  $R'$  were 0.049 and 0.067 respectively. Neutral atom scattering factors were taken from Cromer and Waber [15]. All calculations were performed using TEXSAN [16]. (See Table 1.)

## 3. Results and discussion

### 3.1. X-ray crystal structure of complex $1 \cdot \text{CHCl}_3$

The crystal structure consists of  $[\text{Mn}_2(\text{bomp})(\text{PhCO}_2)_2]^+$  complex cations (Fig. 1), tetraphenylborate anions and chloroform molecules in a 1:1:1 molar ratio. Selected distances and angles with their estimated standard deviations are listed in Table 2. The structure of the complex cation is very similar to that of  $[\text{Zn}_2(\text{bomp})(\text{MeCO}_2)_2]^+$ , which has been reported previously [12]. The complex cation consists of one dinucleating ligand  $\text{bomp}^-$ , two manganese(II) ions and two

benzoate groups. The two manganese ions are bridged by the one phenolic oxygen of the dinucleating ligand and the two benzoate ions, forming a  $\mu$ -phenoxo-bis( $\mu$ -benzoato)dimanganese(II) core structure. The  $\text{Mn}(1) \cdots \text{Mn}(2)$  separation is  $3.3892(7) \text{ \AA}$ , which is common for the  $\text{Mn} \cdots \text{Mn}$  distance of  $\mu$ -phenoxo-bis( $\mu$ -carboxylato)dimanganese(II) complexes ( $3.2\text{--}3.6 \text{ \AA}$ ) [11,18–21].

Atom Mn(1) has a six-coordinate distorted octahedral geometry with O(1), O(2), O(3) and N(1) of  $\text{bomp}^-$  and O(6) and O(8) of the two benzoate groups.

Table 1  
Crystallographic data for  $1 \cdot \text{CHCl}_3$

Formula	$\text{C}_{60}\text{H}_{68}\text{BCl}_3\text{Mn}_2\text{N}_2\text{O}_9$
Formula weight	1188.25
Space group	$P2_1/a$ (no. 14)
$a$ ( $\text{\AA}$ )	27.1889(3)
$b$ ( $\text{\AA}$ )	21.5748(3)
$c$ ( $\text{\AA}$ )	10.2173(1)
$\alpha$ ( $^\circ$ )	90
$\beta$ ( $^\circ$ )	96.3749(4)
$\gamma$ ( $^\circ$ )	90
$V$ ( $\text{\AA}^3$ )	5956.4(1)
$Z$	8
$r_{\text{calc}}$ ( $\text{g cm}^{-3}$ )	1.325
Crystal size (mm)	$0.45 \times 0.20 \times 0.20$
$\mu$ (Mo $K\alpha$ ) ( $\text{cm}^{-1}$ )	6.14
$F(000)$	2480.00
$R^a$	0.049
$R'^b$	0.067

$$^a R = \frac{\sum ||F_o| - |F_c||}{\sum |F_o|}$$

$$^b R' = \frac{\sum w(|F_o| - |F_c|)^2}{\sum w|F_o|^2}^{1/2}$$

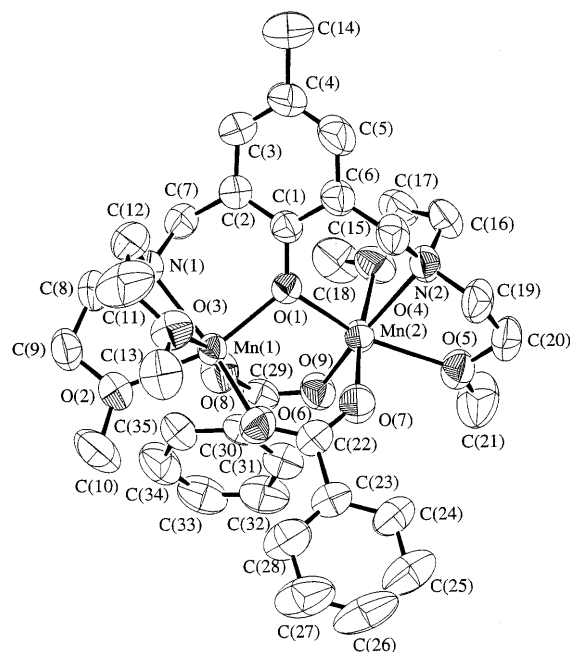


Fig. 1. An ORTEP [17] view of the complex cation  $[\text{Mn}_2(\text{bomp})(\text{PhCO}_2)_2]^+$  with the atom numbering scheme.

The co-ordination geometry around Mn(2) is also distorted octahedral with O(1), O(4), O(5) and N(2) of  $\text{bomp}^-$  and O(7) and O(9) of the two benzoate groups. The geometries around Mn(1) and Mn(2) are very similar to each other, and the complex cation has a pseudo- $C_2$  axis along C(14), C(4), C(1) and O(1). The least-squares plane of the aromatic ring of  $\text{bomp}^-$  and the plane defined by Mn(1), Mn(2) and O(1) are twisted with a dihedral angle of  $44.7^\circ$ .

The dinucleating ligand  $\text{bomp}^-$  has approximately  $C_2$  symmetry, and it has a rigid phenolate head unit, two flexible amine shoulders and four flexible methoxyethyl chelating arms. Owing to the nature of ether oxygen and saturated chelating moieties, two co-ordination sites of  $\text{bomp}^-$  are larger than those of related dinucleating ligands containing Schiff bases or aromatic rings in their structures. Although the co-ordination sites around phenolate and amines of  $\text{bomp}^-$  are slightly too large for divalent transition metal ions, the phenol ring is wound around the pseudo- $C_2$  axis to embrace the chelating arms, and the two metal ions are incorporated. This phenomenon is significant in the dimanganese(II) complex  $[\text{Mn}_2\text{L}(\text{PhCO}_2)_2(\text{NCS})(\text{MeOH})]$ , where  $\text{L}^-$  is 2,6-bis{[*N*-(dimethylaminoethyl)-*N*-methyl]aminomethyl}-4-methylphenolate(1 -) [20]. The twisting dihedral angle for it is  $55^\circ$ .

In the case of the zinc complex  $[\text{Zn}_2(\text{bomp})(\text{MeCO}_2)_2]\text{BPh}_4$ , the bond distances between zinc atoms and axial ether oxygen atoms [2.362(4)–2.440(3) Å] are longer than those between zinc atoms and equatorial ether oxygen atoms [2.197(3)–2.214(5) Å] [12]. However, in the case of complex **1**, the bond distances between manganese atoms and axial ether oxygen atoms [2.275(3)–2.298(3) Å] are almost the same as those between manganese atoms and equatorial ether oxygen atoms [2.290(3)–2.324(3) Å].

The chelating structure of the complex cation of **1**,  $[\text{Mn}_2(\text{bomp})(\text{PhCO}_2)_2]^+$ , is topologically the same as those of the dimanganese complexes of  $\text{bpmp}^-$  [11]. Although the crystal structure of the dimanganese(II,III) complex of  $\text{bpmp}^-$ ,  $[\text{Mn}_2\text{bpmp}(\text{PhCO}_2)_2](\text{ClO}_4)_2 \cdot \text{H}_2\text{O}$ , has been determined, the structure of the corresponding dimanganese(II,II) complex has not been obtained. As far as we know, complex **1** is the first crystallographically characterized dimanganese(II,II) complex with this chelating structure topology.

### 3.2. Magnetic susceptibility of complexes **1–3**

Magnetic susceptibility measurements for manganese complexes **1–3** were made on polycrystalline samples in the temperature range 1.8–300 K. The  $\mu_{\text{eff}}$  values per Mn(II) of the complexes at room temperature are in the range 5.45–5.50  $\mu_{\text{B}}$  (Table 3), which is slightly lower than the spin-only value of high-spin Mn(II) (5.92  $\mu_{\text{B}}$ ).

The magnetic moments decrease with decreasing temperature, suggesting an antiferromagnetic interaction within a pair of Mn(II) ions. The temperature dependencies of  $\chi_{\text{A}}$  and  $\mu_{\text{eff}}$  per Mn for **1** are shown in Fig. 2. The magnetic susceptibility equation for the dinuclear manganese(II) system based on the isotropic Heisenberg model  $\mathcal{H} = -2JS_1 \cdot S_2$  ( $S_1 = S_2 = 5/2$ ) is given by Eq. (1):

$$\chi_{\text{A}} = \frac{Ng^2\beta^2}{kT} \cdot \frac{x^{28} + 5x^{24} + 14x^{18} + 30x^{10} + 55}{x^{30} + 3x^{28} + 5x^{24} + 7x^{18} + 9x^{10} + 11} + N\alpha \quad (1)$$

where  $x = \exp(-J/kT)$ , and the other symbols have their usual meanings. The cryomagnetic properties of **1** are simulated well by Eq. (1) using the magnetic parameters  $g = 2.00$ ,  $J = -4.5 \text{ cm}^{-1}$  and  $N\alpha = 0$ . The reliability factor, defined as  $R(\mu) = \Sigma(\mu_{\text{obs}} - \mu_{\text{cal}})^2 / \Sigma(\mu_{\text{obs}})^2$ , is  $2.5 \times 10^{-5}$ . Similarly, good magnetic simulations have been attained for **2** and **3**. The best-fitting parameters obtained for these complexes are

Table 2  
Selected distances (Å) and angles ( $^\circ$ ) for complex **1**·CHCl<sub>3</sub>

Mn(1)–O(1)	2.103(2)	Mn(2)–O(1)	2.106(2)
Mn(1)–O(2)	2.290(3)	Mn(2)–O(4)	2.324(3)
Mn(1)–O(3)	2.298(3)	Mn(2)–O(5)	2.275(3)
Mn(1)–O(6)	2.085(3)	Mn(2)–O(7)	2.124(3)
Mn(1)–O(8)	2.130(3)	Mn(2)–O(9)	2.095(3)
Mn(1)–N(1)	2.271(3)	Mn(2)–N(2)	2.286(3)
Mn(1)⋯Mn(2)	3.3892(7)		
O(1)–Mn(1)–O(2)	159.6(1)	O(1)–Mn(2)–O(4)	94.6(1)
O(1)–Mn(1)–O(3)	105.3(1)	O(1)–Mn(2)–O(5)	159.5(1)
O(1)–Mn(1)–O(6)	100.4(1)	O(1)–Mn(2)–O(7)	91.4(1)
O(1)–Mn(1)–O(8)	89.8(1)	O(1)–Mn(2)–O(9)	105.2(1)
O(1)–Mn(1)–N(1)	87.4(1)	O(1)–Mn(2)–N(2)	87.4(1)
O(2)–Mn(1)–O(3)	81.2(1)	O(4)–Mn(2)–O(5)	87.7(1)
O(2)–Mn(1)–O(6)	99.1(1)	O(4)–Mn(2)–O(7)	173.0(1)
O(2)–Mn(1)–O(8)	81.4(1)	O(4)–Mn(2)–O(9)	87.0(1)
O(2)–Mn(1)–N(1)	75.5(1)	O(4)–Mn(2)–N(2)	73.7(1)
O(3)–Mn(1)–O(6)	88.5(1)	O(5)–Mn(2)–O(7)	85.4(1)
O(3)–Mn(1)–O(8)	162.0(1)	O(5)–Mn(2)–O(9)	95.3(1)
O(3)–Mn(1)–N(1)	74.4(1)	O(5)–Mn(2)–N(2)	73.7(1)
O(6)–Mn(1)–O(8)	98.6(1)	O(7)–Mn(2)–O(9)	95.0(1)
O(6)–Mn(1)–N(1)	162.6(1)	O(7)–Mn(2)–N(2)	102.9(1)
O(8)–Mn(1)–N(1)	96.9(1)	O(9)–Mn(2)–N(2)	157.9(1)
Mn(1)–O(1)–Mn(2)	107.3(1)		

Table 3  
Magnetic data for complexes **1–3**<sup>a</sup>

Complex	$\mu_{\text{eff}}$ ( $\mu_{\text{B}}$ ) <sup>b</sup>	$J$ ( $\text{cm}^{-1}$ )	$g$	$R(\mu) \times 10^5$
<b>1</b>	5.50	–4.5	2.00	2.5
<b>2</b>	5.48	–5.5	2.00	4.6
<b>3</b>	5.46	–5.3	2.00	12.8

<sup>a</sup>  $N\alpha$  assumed to be zero.

<sup>b</sup> At room temperature.

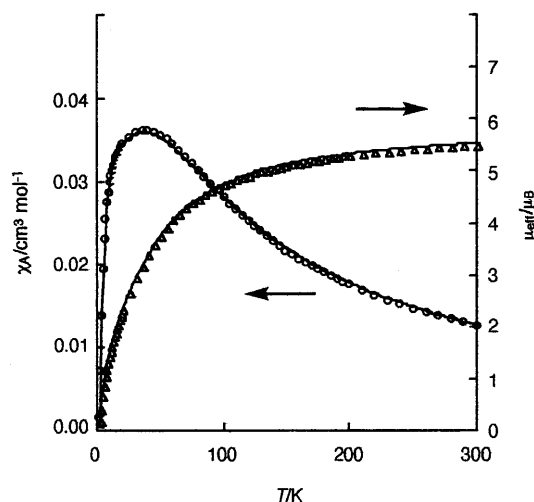


Fig. 2. Temperature dependences of  $\chi_A$  (○) and  $\mu_{\text{eff}}$  (△) of complex **1**. Solid curves are based on Eq. (1), using  $J = -4.5 \text{ cm}^{-1}$ ,  $g = 2.00$  and  $N\alpha = 0 \text{ cm}^3 \text{ mol}^{-1}$ .

summarized in Table 3. The  $J$  values are negative in sign and comparable to those of other  $\mu$ -phenoxo-bis( $\mu$ -carboxylato)dimanganese(II) complexes ( $-2$  to  $-5 \text{ cm}^{-1}$ ) [11,18–21].

### 3.3. Other physicochemical properties in the solid state

The IR spectra of complexes **1–4** show the antisymmetric and symmetric  $\nu(\text{CO}_2)$  vibrations of the carboxylate group at  $1560\text{--}1590$  and  $1400\text{--}1420 \text{ cm}^{-1}$ , respectively. The  $\Delta\nu$  values [ $\Delta\nu = \nu_{\text{as}}(\text{CO}_2) - \nu_{\text{s}}(\text{CO}_2)$ ] are smaller than  $200 \text{ cm}^{-1}$  ( $1400\text{--}1420 \text{ cm}^{-1}$ ), and they are typical of the bridging carboxylate group [22]. This is consistent with the fact that **1** has a  $\mu$ -phenoxo-bis( $\mu$ -benzoato)dimanganese(II) core structure shown using X-ray crystallography. Complexes **1–4** are white and have no absorption bands in the visible region, in accordance with the high-spin  $d^5$  electronic configuration of the Mn(II) ion for **1–3** and with the  $d^{10}$  electronic configuration of the Zn(II) ion for **4**. Judging from the crystal structure and the other physicochemical properties in the solid state, the manganese complexes **1–3** and the zinc complex **4** have similar carboxylato bridging systems to form the  $\mu$ -phenoxo-bis( $\mu$ -carboxylato)dimanganese(II) complexes and the  $\mu$ -phenoxo-bis( $\mu$ -carboxylato)dizinc(II) complex respectively.

### 3.4. Properties and structure in solution

The molar conductances of complexes **1–4** measured in dmf indicate that they act as 1:1 electrolytes in dmf, suggesting the dissociation of counter anions ( $\text{BPh}_4^-$  for **1** and **2**,  $\text{PF}_6^-$  for **3** and **4**). In the FAB mass spectra of **1** and **3** in dmf, the most predominant ion appeared at  $m/z$  625, corresponding to  $[\text{Mn}_2(\text{bomp})-$

$(\text{PhCO}_2)_2]^+$  ( $\text{C}_{35}\text{H}_{47}\text{Mn}_2\text{N}_2\text{O}_9$ ). In the case of **2**, the signal of  $[\text{Mn}_2(\text{bomp})(\text{MeCO}_2)_2]^+$  ( $\text{C}_{25}\text{H}_{43}\text{Mn}_2\text{N}_2\text{O}_9$ ) appeared at  $m/z$  749 as the main peak. In the spectrum of the zinc complex **4**, the most predominant ions appeared at  $m/z$  767, 769 and 771. The isotope pattern around  $m/z$  771 corresponds to  $[\text{Zn}_2(\text{bomp})(\text{PhCO}_2)_2]^+$  ( $\text{C}_{35}\text{H}_{47}\text{N}_2\text{O}_9\text{Zn}_2$ ). These results indicate that the counter anions dissociate in dmf, but the structures of the complex cations are maintained in dmf. In the  $^1\text{H}$  and  $^{13}\text{C}$  NMR of **4**, signals of the four chelating arms are broad due to the interconversion between axial and equatorial chelating arms. This indicates the co-ordination of methoxyethyl chelating arms to Mn(II) centers.

### 3.5. Electrochemistry

Typical cyclic voltammograms of **3** and **4** in  $\text{CH}_3\text{CN}$  at  $25^\circ\text{C}$  are shown in Fig. 3. Electrochemical data for the complexes are given in Table 4. The voltam-

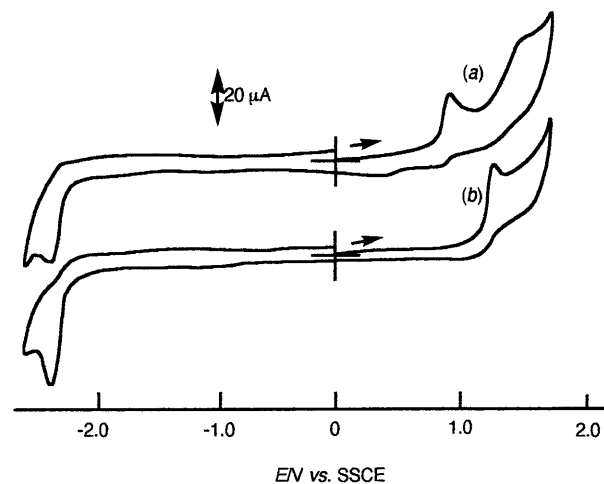


Fig. 3. Cyclic voltammograms of the complexes (a) **3** and (b) **4** in MeCN at a scan rate of  $100 \text{ mV s}^{-1}$ .

Table 4  
Electrochemical data for complexes **3** and **4**

Complex	$E^{\circ}$ (V) versus SSCE <sup>a</sup>	$\Delta E$ (mV) <sup>b</sup>	$I_{\text{pc}}$ (U) <sup>c</sup>	$I_{\text{pa}}/I_{\text{pc}}$ <sup>d</sup>
(A) Reduction				
<b>3</b>	-2.39	irrev.	1790	irrev.
<b>4</b>	-2.38	irrev.	2280	irrev.
(B) Oxidation				
<b>3</b>	+0.92	100	983	0.77
<b>4</b>	+1.28	102	1340	0.78

<sup>a</sup>  $E^{\circ} = (E_{\text{pc}} + E_{\text{pa}})/2$ .

<sup>b</sup> Scan rate:  $500 \text{ mV s}^{-1}$ .

<sup>c</sup> Peak current parameters at  $100 \text{ mV s}^{-1}$ .  $U = \mu\text{As}^{1/2} \text{ V}^{-1/2} \text{ cm}^{-2} \text{ mM}^{-1}$ .

<sup>d</sup> Peak current ratios at  $500 \text{ mV s}^{-1}$ .

mograms of the manganese complex **3** reveal a reduction process at  $-2.4$  V and an oxidation process at  $+0.9$  V versus SSCE (Fig. 3(a)). In contrast to the voltammogram of the corresponding zinc complex **4**, whose reduction and oxidation processes should be ascribed to the ligand-centered electron transfer of bomp in the complex cation, the reduction process of **3** at  $-2.4$  V versus SSCE is caused by the reduction of bomp in the complex cation. On the other hand, the oxidation process at  $+0.9$  V corresponds to the oxidation of Mn(II). This is tentatively assigned to  $\text{Mn}^{\text{II}}\text{Mn}^{\text{II}}/\text{Mn}^{\text{II}}\text{Mn}^{\text{III}}$ , although coulometry has not been successful. The oxidation process of **3** is irreversible at a scan rate of  $100 \text{ mV s}^{-1}$ , but it becomes quasi-reversible at a faster scan rate of  $500 \text{ mV s}^{-1}$ . This indicates that the one-electron oxidation product  $[\text{Mn}^{\text{II}}\text{Mn}^{\text{III}}(\text{bomp})(\text{PhCO}_2)_2]^{2+}$  is not stable and a subsequent homogeneous chemical reaction occurs. The formal reduction potential ( $E^\circ$ ) for the oxidation of the complex cation  $[\text{Mn}_2(\text{bomp})(\text{PhCO}_2)_2]^+$  corresponding to  $\text{Mn}^{\text{II}}\text{Mn}^{\text{II}}/\text{Mn}^{\text{II}}\text{Mn}^{\text{III}}$  couple is  $0.92$  V. This value is higher than that of  $[\text{Mn}_2\text{bomp}(\text{PhCO}_2)_2](\text{ClO}_4)_2 \cdot \text{H}_2\text{O}$  ( $\sim 0.5$  V) and than those of other  $\mu$ -phenoxo-bis( $\mu$ -carboxylato)dimanganese(II) complexes of acyclic dinucleating ligands ( $0.45$ – $0.65$  V) [11,19,20]. This is because the co-ordination site of  $\text{bomp}^-$  is not suitable for incorporating smaller Mn(III) ions.

#### 4. Conclusion

In this study, three new dinuclear manganese(II) complexes are reported. The dinucleating ligand  $\text{bomp}^-$  was shown to incorporate a  $\mu$ -phenoxo-bis( $\mu$ -carboxylato)dimanganese(II) core. The Mn(II) ions in the complex cation were much more difficult to oxidize than the other related dimanganese(II) complexes due to the large co-ordination sites containing the methoxy groups and saturated chelate chains.

#### Acknowledgements

We are grateful to Miss Tomoko Koide of the Institute for Life Support Technology, Yamagata Technopolis Foundation, for the help in FAB mass spectrometrical measurements, and Miss Rie Itoh for the help in molar conductance measurements.

#### References

- [1] (a) Y. Kono, I. Fridovich, *J. Biol. Chem.* 258 (1983) 6015. (b) Y. Kono, I. Fridovich, *J. Biol. Chem.* 258 (1983) 13 646.
- [2] G.S. Allgood, J.J. Perry, *J. Bacteriol.* 168 (1986) 563.
- [3] (a) V.V. Barynin, A.I. Grebenko, *Dokl. Akad. Nauk SSSR* 286 (1986) 461. (b) S.V. Khangulov, M.G. Goldfeld, V.V. Gerasimenko, N.E. Andreeva, V.V. Barynin, A.I. Grebenko, *J. Inorg. Biochem.* 40 (1990) 279.
- [4] M. Kagawa, N. Murakoshi, Y. Nishikawa, G. Matsumoto, Y. Kurata, T. Mizobata, Y. Kawata, J. Nagai, *Arch. Biochem. Biophys.* 362 (1990) 346.
- [5] A. Willing, H. Follmann, G. Auling, *Eur. J. Biochem.* 170 (1988) 603.
- [6] R.S. Reczkowski, D.E. Ash, *J. Am. Chem. Soc.* 114 (1992) 10 992.
- [7] R. Cammack, A. Chapmann, W.-P. Lu, A.A. Karagouni, D.P. Kelly, *FEBS Lett.* 252 (1989) 239.
- [8] (a) H.L. Carrel, J.P. Glusker, V. Burger, F. Manfre, D. Tritsch, J.-F. Biellmann, *Proc. Natl. Acad. Sci. U. S. A.* 86 (1989) 4440. (b) M. Whitlow, A.J. Howard, B.C. Finzel, T.L. Poulos, E. Winborne, G.L. Gilliland, *Proteins* 9 (1991) 153. (c) C.A. Collyer, K. Henrick, D.M. Blow, *J. Mol. Biol.* 212 (1990) 211.
- [9] J.F. Davies, Z. II. Hostomka, Z. Hostomsky, S.R. Jordan, D.A. Matthews, *Science* 252 (1991) 88.
- [10] M.C. Wilce, C.S. Bond, N.E. Dixon, H.C. Freeman, J.M. Guss, P.E. Lilley, J.A. Wilce, *Proc. Natl. Acad. Sci. U. S. A.* 95 (1998) 3472.
- [11] M. Suzuki, M. Mikuriya, S. Murata, A. Uehara, H. Oshio, S. Kida, K. Saito, *Bull. Chem. Soc. Jpn.* 60 (1987) 4305.
- [12] H. Sakiyama, R. Mochizuki, A. Sugawara, M. Sakamoto, Y. Nishida, M. Yamasaki, *J. Chem. Soc., Dalton Trans.* (1999) 997.
- [13] A. Altomare, M.C. Burla, M. Camalli, M. Cascarano, C. Giacovazzo, A. Guagliardi, G. Polidori, *J. Appl. Crystallogr.* 27 (1994) 435.
- [14] P.T. Beurskens, G. Admiraal, G. Beurskenes, W.P. Bosman, R. de Geder, R. Israel, J.M.M. Smits, The DIRDIF-94 program system, Technical Report of the Crystallography Laboratory, University of Nijmegen, The Netherlands, 1994.
- [15] D.T. Cromer, J.T. Waber, *International Tables for X-Ray Crystallography*, vol. IV, Kynoch Press, Birmingham, UK, 1974 Table 2.2 A.
- [16] TEXSAN, Crystal Structure Analysis Package, Molecular Structure Corporation, Houston, TX, 1985 and 1992.
- [17] C.K. Johnson, ORTEP, Report ORNL 5138, Oak Ridge National Laboratory, Oak Ridge, TN, 1976.
- [18] H. Sakiyama, H. Tamaki, M. Kodera, N. Matsumoto, H. Ōkawa, *J. Chem. Soc., Dalton Trans.* (1993) 591.
- [19] C. Higuchi, H. Sakiyama, H. Ōkawa, R. Isobe, D.E. Fenton, *J. Chem. Soc., Dalton Trans.* (1994) 1097.
- [20] C. Higuchi, H. Sakiyama, H. Ōkawa, D.E. Fenton, *J. Chem. Soc., Dalton Trans.* (1995) 4015.
- [21] M. Mikuriya, T. Fujii, S. Kamisawa, Y. Kawasaki, T. Tokii, H. Oshio, *Chem. Lett.* (1990) 1181.
- [22] G.B. Deacon, R.J. Phillips, *Coord. Chem. Rev.* 32 (1980) 227.